A general approach to prepare conjugated polymer dot embedded silica nanoparticles with a SiO2@CP@SiO2 structure for targeted HER2-positive cellular imaging

ARTICLE *in* NANOSCALE · JULY 2013

Impact Factor: 7.39 · DOI: 10.1039/c3nr02390g · Source: PubMed

5 AUTHORS, INCLUDING:

Junlong Geng
Institute of Materials research & engineering
38 PUBLICATIONS **781** CITATIONS
SEE PROFILE

Jing Liang
National University of Singapore
20 PUBLICATIONS **281** CITATIONS
SEE PROFILE

Haibin Shi
Stanford University
20 PUBLICATIONS **566** CITATIONS
SEE PROFILE

Bin Liu
National University of Singapore
389 PUBLICATIONS **9,011** CITATIONS
SEE PROFILE

Nanoscale

RSC Publishing

PAPER

View Article Online
View Journal | View Issue

A general approach to prepare conjugated polymer dot embedded silica nanoparticles with a SiO_2@CP@SiO_2 structure for targeted HER2-positive cellular imaging†

Cite this: *Nanoscale*, 2013, **5**, 8593

Junlong Geng,[a] Jie Liu,[a] Jing Liang,[a] Haibin Shi[a] and Bin Liu*[ab]

We report on a one-step synthesis of conjugated polymer (CP) embedded silica nanoparticles (NPs) with a SiO_2@CP@SiO_2 structure by combination of a precipitation method and a modified Stöber approach. Four types of CPs are employed to demonstrate the versatility of the developed strategy, yielding fluorescent silica NPs with emission across the visible spectrum. Field emission transmission electron microscopy investigation reveals that the entanglement between hydrophobic CPs and the aminopropyl groups of 3-aminopropyl triethoxysilane contributes to the successful encapsulation of CPs into a silica matrix. The synthesized NPs exhibit excellent physical stability and good photostability. In addition, they have amine groups on surfaces, which benefit further conjugation for biological applications. Through reaction with a peptide (GGHAHFG) that is specific to the HER2 receptor, the synthesized NPs have been successfully applied for targeted cellular imaging of HER2-overexpressed SKBR-3 breast cancer cells. Along with its high quantum yield and benign biocompatibility, the developed CP embedded silica NPs have great potential for applications in biological imaging.

Received 9th May 2013
Accepted 2nd July 2013

DOI: 10.1039/c3nr02390g

www.rsc.org/nanoscale

1 Introduction

The fluorescence microscopy technique has attracted great interest in biological research and cancer diagnosis due to its noninvasive, real time and high resolution characteristics.[1–3] It has been recognized that fluorescent probes with high brightness, good photostability, benign biocompatibility and easy surface functionalization capabilities are beneficial for achieving optimal physiological performance in biological studies. The traditional small fluorophores and fluorescent proteins show small Stokes shift and poor photostability,[4] while semiconductor quantum dots (QDs) exhibit notorious cytotoxicity,[5] all hindering their practical biological applications. Recently, conjugated polymers (CPs) have emerged as effective fluorescent materials due to their distinguished advantages.[6–8] CP based materials show large absorption cross-section, strong fluorescence, high photostability and favourable biocompatibility, which meet the requirements of fluorescent probes for biological applications.[9,10] As the inherent hydrophobic backbones hinder CPs to be soluble in an aqueous environment, strategies to endow CPs with good water solubility or dispersibility are highly desirable.[6,7,10]

So far, three main strategies have been developed to render CPs with good water solubility or dispersibility. One strategy is to graft ionic side chains to CP backbones to yield conjugated polyelectrolytes (CPEs), which can further self-assemble in aqueous media.[6,11] Unfortunately, the generated CPEs often create problems of nonspecific interaction with biosubstrates because of their charged side chains. Another strategy is to prepare cross-linked CP NPs with high stability by click chemistry,[12,13] which involves multiple-step monomer modification. The third strategy is to prepare CP NPs through a precipitation or an emulsion method,[14–19] which requires mixing of an organic phase with an aqueous phase under sonication or magnetic stirring. The CP NPs are formed based on the weak hydrophobic interaction between CPs and a polymer matrix, which could result in low stability in aqueous media for long term studies. In addition, CP NPs prepared *via* a nanoprecipitation or an emulsion method could easily lose their physical stability and may not be redispersed in water after drying.[13] As a result, development of a facile and effective approach for fabricating CP NPs that simultaneously possess good water dispersibility, excellent structural and optical stability and surface functional groups remains challenging.

The pioneering work by Stöber has stimulated the development of silica NPs for a variety of applications in biomedicine and photonics.[20–23] Organic dye doped silica NPs have shown great promise in various biological applications due to their good photostability, excellent brightness and benign

[a]*Department of Chemical and Biomolecular Engineering, National University of Singapore, 117576, Singapore. E-mail: cheliub@nus.edu.sg; Fax: +65 6779-1936*
[b]*Institute of Materials Research Engineering, 3 Research Link, 117602, Singapore*

† Electronic supplementary information (ESI) available: The estimation of PFBT dot molecular weight, PL spectra of four CPs in THF, the fluorescence intensity evolution of SiO_2@PFBT@SiO_2 NPs in PBS buffer, FE-TEM images of PFBT dots and SiO_2@PFBT@SiO_2 NPs with the addition of a 200 μL TEOS precursor, chemical structure and LC-MS characterization of a peptide, 3D CLSM fluorescence image and flow cytometry study. See DOI: 10.1039/c3nr02390g

biocompatibility.[21,23] In view of the notable advantages of a silica matrix, it holds great potential to improve CP NP performance in stability and biocompatibility through encapsulation of CPs in a silica matrix. As the highly hydrophobic CP chains are immiscible with the hydrophilic silica matrix, the encapsulation of CPs in silica NPs generally requires the assistance of block copolymers[24] or tedious modification of CP chains and silanes.[21,23] Although mesoporous silica matrices have also been used to directly encapsulate untreated CPs, the porous structure is unable to protect CPs from the invasion of solvents or oxygen molecules, leading to poor stability for long term biological applications.[25] As a consequence, a more general and straightforward approach to prepare CP embedded silica NPs is still in demand.

In this contribution, we report a general, simple and effective strategy to synthesize CP embedded silica NPs with a unique SiO_2@CP@SiO_2 structure (SiO_2@CP@SiO_2 NPs) by integrating a precipitation method and a modified Stöber approach. This approach allows the encapsulation of CPs inside the silica NPs without sophisticated CP modification or tedious silane monomer conjugation. The obtained SiO_2@CP@SiO_2 NPs not only show high stability but also have surface functionalized amine groups that enable bioconjugation for further biological applications. The formation mechanism of SiO_2@CP@SiO_2 NPs is investigated by field emission transmission electron microscopy (FE-TEM) and their detailed optical properties are also studied. The application of SiO_2@CP@SiO_2 NPs as an effective fluorescent probe is demonstrated by functionalization of NP surfaces with a HER2 specific peptide (GGHAHFG) for targeted cellular imaging using HER2-overexpressed SKBR-3 breast cancer cells as an example. By conjugation of their simple synthetic procedure, high fluorescence quantum yield, excellent physical stability and good photostability, the developed SiO_2@CP@SiO_2 NPs can serve as an efficient fluorescent nanoprobe for biological applications.

2 Results and discussion

2.1 Preparation and characterization of SiO_2@CP@SiO_2 NPs

To synthesize SiO_2@CP@SiO_2 NPs, the THF solution of CP was first poured into an ethanol–water mixture (v/v = 9 : 1) under sonication. Upon magnetic stirring, THF gradually evaporated and CPs formed small CP dots. A silica precursor, tetraethyl orthosilicate (TEOS) as well as an ammonia catalyst were subsequently added to the resulting solution. A sol–gel silica reaction took place in the presence of the CP dots. After 12 h, 3-aminopropyl triethoxysilane (APTES) was then added to modify silica NPs with amine functional groups for further bioconjugation. To the best of our knowledge, this is the first report on the synthesis of SiO_2@CP@SiO_2 NPs at room temperature without specific CP or silane modification.

To demonstrate the versatility of this method for preparation of CP encapsulated silica NPs, four different polymers with various emission colours were chosen in this study. These CPs are poly(9,9′-dihexylfluorene-*alt*-1,4-phenylene) (PFP), poly(9,9′-didehexylfluorenyl divinylene-*alt*-1,4-phenylene) (PFVP), poly(9,9-dihexylfluorene-*alt*-2,1,3-benzothiadiazole) (PFBT) and poly[(9,9-dihexylfluorenyl-*co*-2,1,3-benzothiadiazole)-*co*-4,7-di-(thiophen-2-yl)-2,1,3-benzothiadiazole] (PFBTDBT), respectively, which were synthesized according to our previous reports.[26] The fluorescence emission wavelengths of the CPs are fine-tuned from 400 nm to 850 nm and their chemical structures are shown in Scheme 1.

Fig. 1a shows the UV-vis absorption and fluorescence spectra of the prepared SiO_2@CP@SiO_2 NP aqueous suspensions. The increased baselines of the absorption spectra at the short wavelength are due to the strong scattering of the silica matrix.[21] The emission maxima of PFP-, PFVP-, PFBT- and PFBTDBT encapsulated silica NP suspensions are 421 nm, 482 nm, 554 nm and 699 nm, respectively. The fluorescence spectra of the corresponding CPs in THF are shown in Fig. S1 in the ESI†. It is noted that the emission maxima of PFP–, PFVP–, PFBT– and PFBTDBT–SiO_2 NP suspensions are red-shifted by 8 nm, 12 nm, 11 nm and 41 nm, respectively, as compared to those of pure CPs in THF. The red shifts of the emission maxima of these NPs are mainly derived from the aggregation of CP chains in silica NP formulation, which is consistent with the previous reports of CP NPs prepared through nanoprecipitation and emulsion methods.[18,19,24] In addition, the aqueous suspensions of SiO_2@CP@SiO_2 NPs show bright and vivid colours under the excitation of a hand held UV lamp as shown in Fig. 1b. These results illustrate that the photophysical properties of SiO_2@CP@SiO_2 NPs are tunable by choosing different CPs.

Table 1 shows that the SiO_2@CP@SiO_2 NPs have an average diameter from ~60 to ~70 nm determined by laser light scattering. It has been reported that NPs with a size from 50 nm to

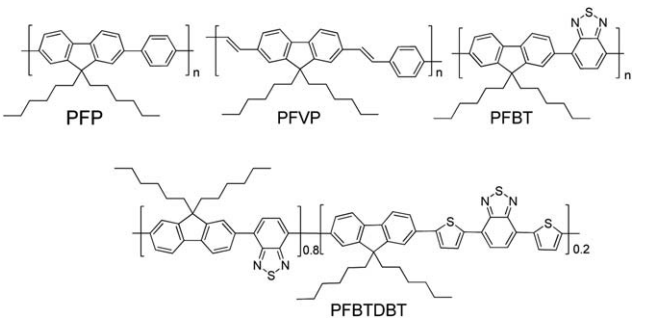

Scheme 1 Chemical structures of four CPs used in this study.

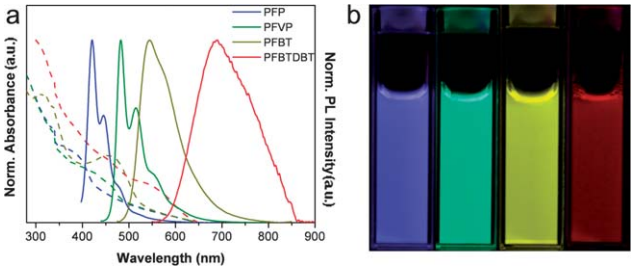

Fig. 1 (a) Normalized UV-vis absorption (dashed line) and PL spectra (solid line) of SiO_2@CP@SiO_2 NPs in water. (b) Photographs of SiO_2@CP@SiO_2 NP suspensions in water under a hand held UV lamp (excited at 365 nm).

Table 1 Characterization of SiO_2@CP@SiO_2 NPs

Loaded CP	PFP	PFVP	PFBT	PFBTDBT
Particle size (nm)	65	62	68	72
Zeta potential (mV)	+26	+23	+25	+25
Encapsulation efficiency (%)	100	100	100	100
Quantum yield[a] (%)	54	35	27	20

[a] The quantum yields of SiO_2@PFP@SiO_2, SiO_2@PFVP@SiO_2, SiO_2@PFBT@SiO_2 and SiO_2@PFBTDBT@SiO_2 NPs were measured using quinine sulfate (0.1 M H_2SO_4; QY = 0.54), fluorescein (0.1 M NaOH; QY = 0.95), 4-(dicyanomethylene)-2-methyl-6-(*p*-dimethylamino-styryl)-4*H*-pyran (methanol; QY = 0.43) as the standard, respectively.

200 nm show good cellular uptake efficiency.[27,28] The zeta potential of SiO_2@CP@SiO_2 NPs was measured to be around +25 mV in a neutral aqueous environment, which is mainly derived from the grafted amine groups on NP surfaces. The positively charged surfaces of SiO_2@CP@SiO_2 NPs guarantee the electrostatic repulsion among particles, leading to a relatively good colloidal stability in water. The encapsulation efficiencies of the four CPs in the silica matrix are calculated from the absorption difference of the CP solution in the ethanol–water mixture prior to encapsulation and that of the supernatant after NP centrifugation, which are almost 100% under our experimental conditions. The quantum yield of each SiO_2@CP@SiO_2 NP was measured using commercial fluorophores as the standard. The relatively high quantum yields (>20%) for these four SiO_2@CP@SiO_2 NPs are comparable with the previously reported water dispersible CP NPs.[10,15,18,24] The fluorescence stability of the obtained SiO_2@CP@SiO_2 NPs was also investigated by monitoring the fluorescence intensity change of SiO_2@PFBT@SiO_2 NPs upon incubation in phosphate buffer saline (PBS) at 37 °C as an example. As shown in Fig. S2 in the ESI,† the fluorescence intensity of the SiO_2@PFBT@SiO_2 NP suspension remains ~92% of its initial value after 5 day incubation in 1× PBS. The excellent physical stability of CP NPs is ascribed to the protection of PFBT from the silica matrix.[21–23] Moreover, the dried SiO_2@CP@SiO_2 NPs can be redispersed easily in ethanol or water due to the robust silica matrix. The high fluorescence quantum yield and outstanding stability of SiO_2@CP@SiO_2 NPs benefit their biological applications.

It is generally observed that silica condensation in the presence of seed particles leads to core/shell morphologies.[29,30] In the case of CPs and the silica hybrid system, it is of interest to investigate the evolution of their structures at various reaction times. Taking PFBT as an example, the morphology and structure changes of CP–silica hybrid composites were studied by FE-TEM. In these experiments, PFBT dots were firstly obtained by the precipitation method combining ultrasonication and solvent evaporation. Upon addition of TEOS, a sol–gel silica reaction proceeded in the suspension of PFBT dots. During the process of silica NP formation, aliquots were taken from the reaction solution at time intervals of 20 min, 40 min, 60 min, 3 h and 12 h after TEOS addition. The FE-TEM samples were prepared by directly dropping the reaction solution onto a copper grid with subsequent drying in a vacuum oven to minimize further TEOS precursor cross-linking. As shown in Fig. 2, at the initial 20 min, small black PFBT dots are adsorbed on the silica NP surfaces. The sizes of PFBT dots and silica NPs are estimated to be ~3 nm and ~27 nm, respectively, from Fig. 2a. The 3 nm PFBT dot should only contain a single polymer chain according to the estimation method described in the ESI.† Each PFBT dot is adsorbed on the silica NP surface to form a PFBT dot-punctuated silica NP structure. This interesting pattern may result from the phase separation between the immiscible PFBT and silica matrix components. The sizes of

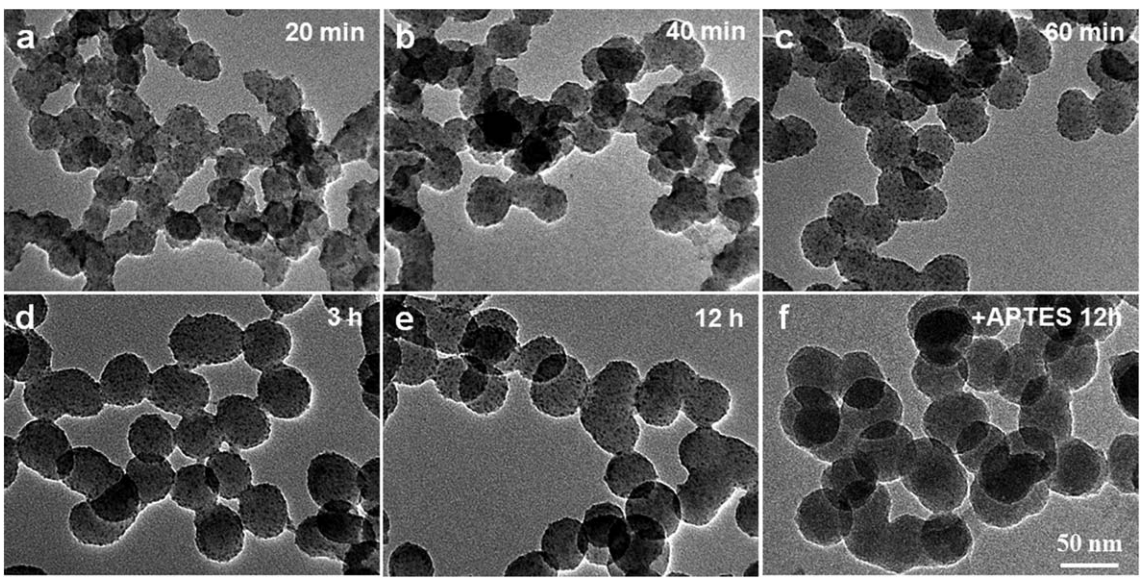

Fig. 2 FE-TEM images of SiO_2@PFBT@SiO_2 NPs taken at different reaction times after adding TEOS (a–e) as well as APTES (f). All images share the same scale bar as that in (f).

silica NPs increase to ~32 nm at 40 min (Fig. 2b) and further increase to ~35 nm (Fig. 2c) and ~42 nm (Fig. 2d) at the time intervals of 1 h and 3 h, respectively. There is little difference in the silica NP size between samples prepared at 3 h and 12 h. During the time interval from 20 min to 12 h, the small black PFBT dots with a size ~3 nm can be clearly observed, further illustrating that hydrophobic PFBT dots cannot be encapsulated into the hydrophilic silica matrix. It is worth noting that PFBT dots are not stable in the absence of the silica matrix. The FE-TEM image of PFBT dots in the ethanol–water mixture without TEOS addition is shown in Fig. S3 in the ESI.† No regular PFBT aggregates are observed in Fig. S3,† indicating that small PFBT dots are not stable and aggregate easily even during the sample preparation. However, the silica substrate provides a robust support for PFBT dots, leading to an observable PFBT dot-punctuated silica NP structure. Interestingly, if SiO_2 NPs and CP dots were synthesized separately, mixed and followed by 12 h stirring, the PFBT dot-punctuated SiO_2 NPs could also be observed (Fig S4 in the ESI†), which further confirm that CP dots tend to be absorbed at the SiO_2 NP surfaces rather than encapsulated inside SiO_2 cores. After reaction for 12 h, APTES was further added into the reaction mixture, which was followed by another 12 h of magnetic stirring. The FE-TEM image of the PFBT–silica mixture after 12 h reaction with APTES is shown in Fig. 2f. An interesting surface morphology evolution from PFBT dot-punctuated silica NP patterns (Fig. 2a–e) to smooth silica NP surfaces (Fig. 2f) is observed. The disappearance of small black PFBT dots after APTES addition illustrates that PFBT dots are more likely encapsulated into the silica matrix upon APTES hydrolysis. It is noted that the size of SiO_2@PFBT@SiO_2 NPs can be easily controlled by changing the amount of the TEOS precursor in the reaction. Doubling the TEOS concentration in the feed will result in an increase in the size of SiO_2@PFBT@SiO_2 NPs from ~40 to ~65 nm, as shown in Fig. S5 in the ESI.†

The successful embedment of PFBT dots into silica layers was further confirmed by checking the colours of the precipitates and supernatants after centrifugation. The yellow precipitate and a clear supernatant are obtained by centrifugation of the reaction solution upon addition of APTES after 12 h reaction, which is shown in the inset of Fig. 3a. After washing five times, the yellow colour is still present in the precipitate (Fig. 3b, inset), indicating that PFBT is stably embedded in silica NPs upon APTES cross-linking. However, addition of TEOS into the PFBT dot-punctuated silica NP suspension followed by 12 h reaction cannot encapsulate PFBT dots in the silica matrix and the supernatant remains yellow (Fig. 3c, inset). In fact, black PFBT dots are separated from silica NPs upon sonication/centrifugation washing as shown in Fig. 3c. Further washing will only lead to clean silica NPs as white precipitates (the inset of Fig. 3d). These data not only illustrate that CP dots cannot be embedded by further addition of TEOS reagents, but also indicate that CP dots adsorbed on silica surfaces are not stable and can be easily removed by sonication/centrifugation treatment. The other three CPs including PFP, PFVP and PFBTDBT can also be embedded into silica NPs with the assistance of APTES reagents (data not shown). Based on FE-TEM images

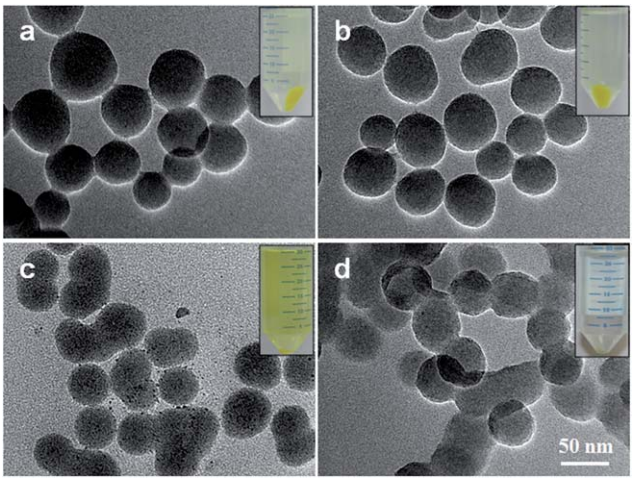

Fig. 3 FE-TEM images of SiO_2@PFBT@SiO_2 NPs with the addition of APTES (upper row; a and b) or TEOS (bottom row; c and d) for a further 12 h reaction followed by centrifuging once (a and c) and five times (b and d). The insets show the respective photographs of SiO_2@PFBT@SiO_2 NPs after centrifugation. All images share the same scale bar as that in (d).

from Fig. 2 and 3, a possible mechanism of the formation of SiO_2@CP@SiO_2 NPs has been proposed.

Scheme 2 illustrates our proposed mechanism for the formation of SiO_2@CP@SiO_2 NPs. CP dots are firstly obtained in an ethanol–water mixture (v/v = 9 : 1) through ultrasonication and THF evaporation (Scheme 2a). Due to the low solubility of hydrophobic backbones in the polar ethanol–water mixture, CP dots are obtained upon THF evaporation. After adding TEOS, a sol–gel procedure is performed which may take the present CP dots as nucleation centers.[30] However, the hydrophilic silica component cannot grow homogeneously

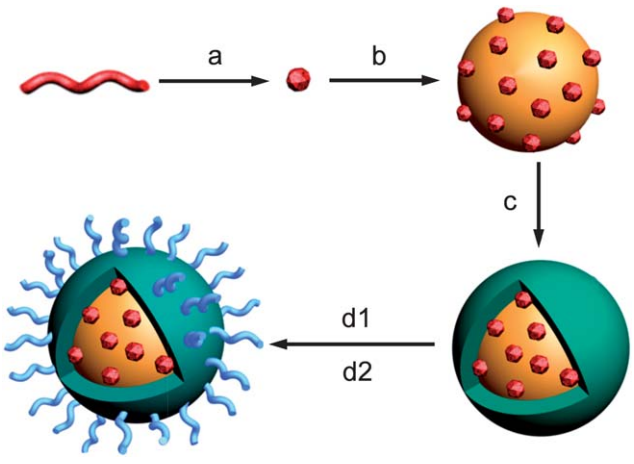

Scheme 2 Schematic illustration of the synthesis of SiO_2@CP@SiO_2 NPs with a surface functionalized targeting peptide. (a) Sonicatioin of a THF solution of CPs in an ethanol–water mixture (v/v = 9 : 1) affords single CP chain dots. (b) Addition of TEOS and ammonia into the CP dots dispersed solution leads to the formation of a CP dot-punctuated silica NP pattern after reaction. (c) Further addition of APTES into the mixture results in CP dots embedded silica NPs with surface functionalized amine groups. (d1) Surface carboxylation with maleic anhydride in the presence of Et_3N. (d2) Peptide conjugation *via* EDC/NHS reaction.

around hydrophobic CP dots due to their different hydrophilicities. On the other hand, the hydrophobic CP dots are not stable in the polar ethanol–water mixtures. To minimize the surface energy, CP dots tend to be adsorbed on the surfaces of the formed silica NPs rather than being encapsulated inside the SiO_2 core (Scheme 2b). As the aminopropyl groups from APTES can entangle with the hydrophobic CP dots, a self-assembled structure with CP dots as the core and triethoxy silane groups pointing outwards is obtained upon APTES addition. The silane groups can further react with other monomers to form a cross-linked network, leading to the encapsulation of CP dots in the silica matrix (Scheme 2c). Moreover, APTES monomers can decorate the surface of SiO_2@CP@SiO_2 NPs with functional amine groups, which facilitate further conjugation with peptides for targeted cellular imaging (Scheme 2d).

2.2 Surface functionalization with a HER2 targeting peptide

To demonstrate the potential of SiO_2@CP@SiO_2 NPs in biological applications, SiO_2@PFBT@SiO_2 NPs were chosen as an example for targeted cellular imaging. As the positively charged amine groups tend to stick to the negatively charged cell membranes,[3,28] we first modified NP surfaces with carboxyl groups using maleic anhydride to minimize the non-specific interaction between NPs and cells. The successful grafting of carboxyl groups on silica NP surfaces was confirmed by the zeta potential measurement. The zeta potential changed from +25 mV for SiO_2@PFBT@SiO_2 NPs with surface functionalized amine groups to −34 mV for SiO_2@PFBT@SiO_2 NPs with surface functionalized carboxyl acid groups (SiO_2@PFBT@SiO_2-COOH NPs). The peptide, GGHAHFG, which can selectively bind to HER2 overexpressed SKBR-3 breast cancer cells was chosen to endow NPs with targeting ability.[31] The amine-bearing GGHAHFG peptide was synthesized by standard solid-phase fluorenylmethoxy carbonyl peptide chemistry.[31] The detailed synthetic procedure is illustrated in the Experimental section and its structure is shown in Scheme S1 in the ESI.† The peptide was further purified by HPLC and characterized by LC-MS (Fig. S6 in ESI†). Subsequent coupling between SiO_2@PFBT@SiO_2-COOH NPs and the peptide *via* the carbodiimide chemistry yielded fluorescent NPs (SiO_2@PFBT@SiO_2-Pep NPs) with targeting ability to HER2 positive cancer cell lines. The zeta potential of SiO_2@PFBT@SiO_2-Pep NPs was further changed to −11 mV, demonstrating the successful coupling between carboxyl groups at the NP surface and amine groups of the peptides.

2.3 Targeted cellular imaging

To examine targeting ability of SiO_2@PFBT@SiO_2-Pep NPs, SiO_2@PFBT@SiO_2-COOH NPs were used as a control in cellular imaging by confocal laser scanning microscopy (CLSM). In these experiments, SKBR-3 breast cancer cells were incubated with both NP suspensions in culture medium for 2 h at 100 μg mL^{-1} NPs. The CLSM images of SKBR-3 breast cancer cells after incubation with both NPs are shown in Fig. 4a and b, respectively. The higher fluorescence intensity in Fig. 4a as compared to that in 4b clearly indicates that the peptide promotes cellular uptake due to the over-expressed HER2 on SKBR-3 breast cancer cell membranes. The low fluorescence intensity from Fig. 4b also illustrates that the carboxyl groups grafted onto the NP surfaces reduce non-specific interactions between NPs and breast cancer cells.[32] It is noted that there is no auto-fluorescence from the control cells without incubation of NPs under the same experimental conditions (Fig. S7 in the ESI†). The 3D image of SKBR-3 cells incubated with SiO_2@PFBT@SiO_2-Pep indicates that NPs are mainly located in the cell cytoplasm as shown in Fig. S8 in the ESI.† As a control, NIH/3T3 fibroblast cells with low HER2 receptors were also incubated with both NP suspensions. The fluorescence intensity from NIH/3T3 cells upon treatment with SiO_2@PFBT@SiO_2-Pep NPs (Fig. 4c) is similar to that from cells upon treatment with SiO_2@PFBT@SiO_2-COOH NPs (Fig. 4d). In addition, the fluorescence intensities shown in Fig. 4c and d are lower than that shown in Fig. 4a. These data indicate the receptor mediated uptake of SiO_2@PFBT@SiO_2-Pep NPs by SKBR-3 breast cancer cells.[2,16,31,33]

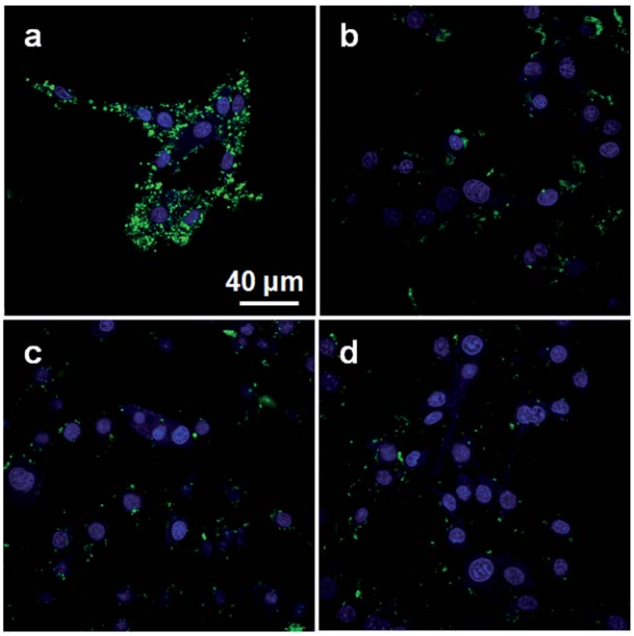

Fig. 4 Confocal fluorescence images of SKBR-3 breast cancer cells after 2 h incubation with (a) SiO_2@PFBT@SiO_2-Pep and (b) SiO_2@PFBT@SiO_2-COOH NP suspensions at 100 μg mL^{-1} NPs at 37 °C. Confocal fluorescence images of NIH/3T3 fibroblast cells after 2 h incubation with (c) SiO_2@PFBT@SiO_2-Pep and (d) SiO_2@PFBT@SiO_2-COOH NP suspensions at 100 μg mL^{-1} NPs at 37 °C. All images have the same scale bar as that in (a).

To obtain quantitative analysis of the targeting effect of the peptides on NP surfaces, flow cytometry was used to evaluate the intracellular fluorescence for SKBR-3 breast cancer cells upon incubation with both NPs. The mean fluorescence intensity of SKBR-3 cells incubated with SiO_2@PFBT@SiO_2-Pep NPs is ~2-fold higher as compared to that upon incubation with SiO_2@PFBT@SiO_2-COOH NPs as shown in Fig. S9 in the ESI.† These data further prove that peptide functionalized NPs favour their cellular uptake by SKBR-3 breast cancer cells due to receptor mediated endocytosis.

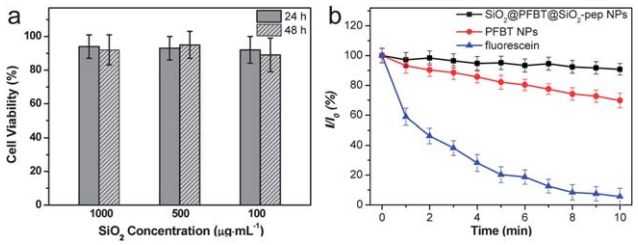

Fig. 5 (a) Metabolic viability of SKBR-3 breast cancer cells after incubation with SiO_2@PFBT@SiO_2-Pep at various NP concentrations for 24 h (gray) and 48 h (shadow). (b) Photostability of SiO_2@PFBT@SiO_2-Pep NPs, PFBT NPs and fluorescein in SKBR-3 breast cancer cells upon continuous laser excitation at 488 nm for 10 min. I_0 is the initial fluorescence intensity and I is the fluorescence intensity of the sample at different time points after illumination.

2.4 Cytotoxicity and photostability

The cytotoxicity of the SiO_2@PFBT@SiO_2-Pep NPs was evaluated by the metabolic viability of NIH/3T3 fibroblast cells after incubation with NP suspensions at 100, 500 and 1000 μg mL^{-1} NPs for 24 h and 48 h, respectively. As shown in Fig. 5a, the cell viabilities remain ~90% upon incubation with SiO_2@PFBT@SiO_2-Pep NP suspensions for 48 h at 1000 μg mL^{-1} NP, a concentration that is 10-fold higher than that used for imaging. These results indicate the low cytotoxicity of the probe, which is ideal for targeted cellular imaging. The photostability of SiO_2@CP@SiO_2-Pep NPs in the cellular environment was also investigated using SiO_2@PFBT@SiO_2-Pep NPs as an example under continuous laser scanning upon excitation at 488 nm. And the results were compared with those of fluorescein and PFBT NPs prepared with a typical precipitation method. The photostability results for SiO_2@PFBT@SiO_2-Pep NPs, PFBT NPs and fluorescein are shown in Fig. 5b. After 10 min of continuous laser illumination, the fluorescence intensity from SKBR-3 breast cells incubated with SiO_2@PFBT@SiO_2-Pep NPs decreases ~9%, which is obviously better than that for PFBT NPs. Under the same conditions, the fluorescence intensity of fluorescein is almost completely quenched by laser illumination. The improved photostability for PFBT–SiO_2-Pep NPs as compared to that for PFBT NPs is expected to result from the robust silica matrix protection, which is beneficial for long term bioimaging studies.

3 Conclusion

In summary, we developed a simple yet effective strategy to prepare CP embedded NPs with a unique SiO_2@PFBT@SiO_2 structure *via* an integration of the precipitation method and a modified Stöber approach. Through FE-TEM investigation of the sample aliquots at various reaction times, the morphology change from CP dot-punctuated silica NPs to CP embedded silica NPs with smooth surfaces was observed. The successful encapsulation of CPs into the silica matrix results from the entanglement between hydrophobic CP chains and APTES reagents. The as-prepared NPs exhibit high quantum yield, excellent photostability, low cytotoxicity and surface available functional groups, benefiting their conjugation with targeting ligands. By conjugation with a specific targeting peptide, the obtained nanoparticles also allow targeted imaging of SKBR-3 breast cancer cells in a high contrast manner. Based on the developed strategy for simple synthesis of SiO_2@CP@SiO_2 NPs, further encapsulation of metal NPs into the silica core can easily lead to nanocomposites with metal enhanced fluorescence.[34] Furthermore, the incorporation of magnetic NPs could afford multimodal nanocomposites with imaging and therapeutic functions,[17,35] which may further broaden the CP based material in theranostic applications.

4 Experimental section

4.1 Materials

Poly(9,9′-dihexylfluorene-*alt*-1,4-phenylene) (PFP), poly(9,9′-didehexylfluorenyl divinylene-*alt*-1,4-phenylene) (PFVP), poly(9,9-dihexylfluorene-*alt*-2,1,3-benzothiadiazole) (PFBT) and poly[(9,9-dihexylfluorenyl-*co*-2,1,3-benzothiadiazole)-*co*-4,7-di(thiophen-2-yl)-2,1,3-benzothadiazole] (PFBTDBT) were synthesized according to the previous reports.[26] Tetraethyl orthosilicate (TEOS), 3-aminopropyl triethoxysilane (APTES), 1-ethyl-3-[3-dimethylaminopropyl] carbodiimide hydrochloride (EDAC), *N*-hydroxysulfosuccinimide (Sulfo-NHS), trifluoroacetic acid (TFA), *N*,*N*-diisopropylethylamine (DIEA), acetic anhydride (Ac_2O), triisopropylsilane (TIS), 4′,6-diamidino-2-phenylindole (DAPI), quinine sulphate, fluorescein, 4-(dicyanomethylene)-2-methyl-6-(*p*-dimethylamino-styryl)-4*H*-pyran, 3-(4,5-dimethylthiazol-2-yl)-2,5-diphenyl tetrazolium bromide (MTT), penicillin–streptomycin solution and dimethyl sulfoxide (DMSO) were purchased from Sigma-Aldrich. Dulbecco's Modified Eagle's Medium (DMEM), fetal bovine serum (FBS) and trypsin–EDTA solution were purchased from Gibco (Lige Technologies, Ag, Switzerland). Hexane, dichloromethane (DCM), dimethylformamide (DMF), ethanol, methanol, tetrahydrofuran (THF), concentrated sulphuric acid and ammonia solution were obtained from Merck (Germany). Rink-amide resin, *O*-benzotriazole-*N*,*N*,*N*′,*N*′-tetramethyl-uronium-hexafluoro-phosphate (HBTU), *N*-hydroxybenzotriazole (HOBt) and Fmoc-protective amino acids were purchased from GL Biochem Ltd. Milli-Q water was supplied by a Milli-Q Plus System (Millipore Corporation, Breford, USA). SKBR-3 breast cancer cells and NIH/3T3 fibroblast cells were provided by American Type Culture Collection.

4.2 Characterization

The UV-vis absorption spectra of CP solutions and their corresponding NPs were measured using a Shimadzu UV-1700 spectrophotometer. Their fluorescence spectra were measured using a fluorometer (LS-55, Perkin Elmer, USA). The average particle sizes and size distributions were determined by laser light scattering with a particle size analyzer (90 Plus, Brookhaven Instruments Co. USA) at a fixed angle of 90° at room temperature. The surface morphologies of SiO_2@CP@SiO_2-NPs were studied by field emission transmission electron microscopy (FE-TEM) (JEM-2010F, JEOL, Japan). The zeta potential was

measured using a zeta potential analyzer (ZetaPlus, Brookhaven Instruments Co., USA) at room temperature.

4.3 Preparation of SiO_2@CP@SiO_2 NPs

The SiO_2@CP@SiO_2 NPs were prepared by the combination of a precipitation method and a modified Stöber approach. Typically, a THF solution (0.3 mL) containing CP (0.15 mg) was poured into a mixture of ethanol and water (v/v = 9 : 1, 10 mL) under sonication using a microtip probe sonicator (XL2000, Misonix Incorporated, NY) for 2 min. The solution was then stirred at room temperature for 2 h to evaporate THF. Subsequently, 100 μL of TEOS was added into the mixture followed by 300 μL of ~30% ammonium solution. The solution was further stirred for 12 h at room temperature. To investigate the evolution mechanism of the formed NPs, aliquots were taken from the solution at different time points to conduct FE-TEM measurements. Then, 40 μL of APTES was added into the above reaction mixture and stirred for another 12 h. The formed SiO_2@CP@SiO_2-NPs were then centrifuged for 10 min at 7500 rpm and washed with ethanol five times to remove ammonia and impurities. In between the washing steps, SiO_2@CP@SiO_2 NPs were redispersed by sonication.

4.4 Synthesis, purification, and characterization of peptide (GGHAHFG)

GGHAHFG was synthesized using a standard Fmoc strategy with rink amide resin as the solid support.[36] The standard HOBT/HBTU/DIEA coupling method was used throughout the whole process. The resin (100 mg, loading ~0.5 mmol g^{-1}) was swelled in HPLC-grade DMF for 1 h at room temperature. Subsequently, the Fmoc group was deprotected in piperidine/DMF (v/v = 1 : 4) for 2 h at room temperature. Following the piperidine removal, the resin was washed extensively with DMF and DCM and dried thoroughly under high vacuum. Next, glycine was dissolved in dry DMF (1.5 mL) together with HBTU (4 equiv.), HOBt (4 equiv.), and DIEA (8 equiv.). The dry resin was then added and the resulting mixture was shaken at room temperature. After overnight reaction, the resin was filtered and washed thoroughly with DMF (3×), DCM (3×) and DMF (3×) until the filtrate became colorless. After drying thoroughly under high vacuum, the resin was deprotected again with 20% piperidine in DMF for the next coupling cycle. The above cycle was repeated until the last amino acid has been coupled. Finally, the resin was capped with a solution of Ac_2O (10 eq.) and DIEA (20 eq.) in DCM (200 mL), and the mixture was allowed to react for 2 h at room temperature. After the whole coupling process, the resin was washed thoroughly with DMF and dried under high vacuum for 2 h at room temperature. The peptide was then cleaved in a mixture of 95% TFA, 2.5% triisopropylsilane (TIS) and 2.5% H_2O for 4 h at room temperature, followed by prolonged concentration in a vacuum until >80% of cleavage cocktail was removed. Cold ether (chilled to 20 °C) was added to the liquid residue to precipitate the peptide. The ether layer was then decanted and the precipitates were dried thoroughly in a vacuum. The resulting peptide was further purified by prep-HPLC and characterized by LC-MS. IT-TOF *m*/*z* calcd: 681.70, found 681.32. The HPLC conditions are: 5–20% B for 10 min, then 20–40% B for 2 min, 5% B for 2 min (Solvent A: 100% H_2O with 0.1% TFA; Solvent B: 100% CH_3CN with 0.1% TFA).

4.5 Preparation of SiO_2@PFBT@SiO_2–Pep NPs

The amine group functionalized SiO_2@PFBT@SiO_2 NPs were firstly modified with maleic anhydride to render carboxyl acid group functionalized SiO_2 NPs. Typically, maleic anhydride (10 mg) in 10 mL of ethanol and 0.5 mL of triethylamine were added into 10 mL of SiO_2@PFBT@SiO_2 NP suspensions and stirred overnight. Then 20 mL of H_2O was added into the mixture, followed by washing with ethanol and H_2O three times, respectively. Subsequently, 3.2 mg of EDAC and 3.6 mg of Sulfo-NHS were added into NP suspension to activate carboxyl groups for 4 h at room temperature. The activated SiO_2 NPs were centrifuged to remove excess ligands and redispersed in 5 mL H_2O. 5 mL of 0.2 M borate buffer was then added to the suspension, which was followed by 0.1 mL of 0.1 M peptide (GGHAHFG). The mixture was stirred at room temperature overnight and then washed with water as well as DMSO to eliminate the excess peptide.

4.6 Preparation of PFBT NPs

PFBT NPs were prepared using a precipitation method.[10] Briefly, a THF solution (1 mL) containing a mixture of PFBT (0.5 mg) was poured into 10 mL of MilliQ water under sonication. THF was then evaporated by magnetic stirring in a fume hood. PFBT NPs were obtained by filtration through a 0.2 μm filter. The quantum yield of PFBT-NPs was estimated to be ~20% using 4-(dicyanomethylene)-2-methyl-6-(*p*-dimethylamino-styryl)-4*H*-pyran in methanol as a standard.

4.7 Cell cultures

SKBR-3 breast cancer cells and NIH/3T3 fibroblast cells were cultured in folate-free DMEM medium containing 10% fetal bovine serum and 1% penicillin–streptomycin at 37 °C in a humidified environment containing 5% CO_2. Before the experiment, the cells were precultured until confluence was reached.

4.8 Cellular imaging

SKBR-3 breast cancer cells were cultured in a chamber (LAB-TEK, Chambered Coverglass System) at 37 °C. After 80% confluence, the medium was removed and the adherent cells were washed three times with 1× phosphate buffer saline (PBS) buffer. SiO_2@PFBT@SiO_2-Pep NP and SiO_2@PFBT@SiO_2-COOH NP suspensions at 100 μg mL^{-1} NPs in FBS free DMEM medium were then added to the chamber. After incubation for 2 h, cells were washed three times with 1× PBS buffer and then fixed by 75% ethanol for 10 min. Subsequently, the cells were incubated with DAPI for 15 min to stain the cell nuclei. The cell monolayer was further washed three times with 1× PBS buffer and imaged by CLSM (Zeiss LSM 410, Jena, Germany) with imaging software (Fluoview FV1000). The confocal images of NIH/3T3 cells treated

with SiO_2@PFBT@SiO_2-Pep SiO_2@PFBT@SiO_2-COOH NPs under the same conditions were also studied.

4.9 Flow cytometry study

Three groups of SKBR-3 breast cancer cells were cultured in a 6-well culture plate to achieve the desired confluence. One group was used as the control without treatment. The other two groups were treated with SiO_2@PFBT@SiO_2-Pep NP and SiO_2@PFBT@SiO_2-COOH NP suspensions at 100 μg mL^{-1} NPs in FBS free DMEM medium, respectively. After incubation for 2 h at 37 °C, the control and sample groups were washed with 1× PBS buffer three times and then treated with 1× PBS trypsin, followed by washing with DMEM medium through centrifugation. MCF-7 breast cancer cells with a density of $\sim 1.5 \times 10^5$ cells per mL were dispersed in the FBS free DMEM medium (2 mL) for both control and sample groups. Flow cytometry measurements were conducted using a Cyan-LX (DakoCytomation). The mean fluorescence was determined by counting 10 000 events (λ_{ex} = 488 nm, 680/40 nm bandpass filter).

4.10 Cytotoxicity of SiO_2@PFBT@SiO_2-Pep NPs

MTT assays were performed to assess the metabolic activity of NIH/3T3 fibroblast cells. NIH/3T3 fibroblast cells were seeded in 96-well plates (Costar, IL, USA) with a density of 4×10^4 cells per mL. After 24 h incubation, the medium was replaced by SiO_2@PFBT@SiO_2-Pep NP suspensions with various NP concentrations (100, 500 and 1000 μg mL^{-1}), and the cells were further incubated for 24 and 48 h, respectively. After the designated time intervals, the wells were washed three times with 1× PBS buffer, and freshly prepared MTT (0.5 mg mL^{-1}) solution (100 μL) in culture medium was added to each well. The MTT medium solution was carefully removed after 3 h incubation in the incubator. DMSO (100 μL) was then added into each well and the plate was gently shaken for 10 min at room temperature to dissolve all precipitates. The absorbance of MTT at 570 nm was monitored by the microplate reader (Genios Tecan) after subtracting the absorbance of the corresponding control cells incubated with SiO_2@PFBT@SiO_2-Pep NPs at the same concentration but without the addition of MTT to eliminate the absorbance interference from PFBT. Cell viability was expressed by the ratio of absolute absorbance of the cells incubated with NP suspensions to that of the cells incubated with culture medium only.

4.11 Photostability of SiO_2@PFBT@SiO_2-Pep NPs

To compare the photostability of SiO_2@PFBT@SiO_2 NPs with that of fluorescein and PFBT NPs, the photostability of SiO_2@PFBT@SiO_2-Pep, PFBT NPs and fluorescein was investigated. SKBR-3 breast cancer cells incubated with SiO_2@PFBT@SiO_2-Pep NPs, PFBT NPs and fluorescein were prepared according to the procedures described above. The CLSM images of the sample were recorded at 1 min interval under continuous laser scanning at an excitation wavelength of 488 nm with a laser power of 4.75 mW. The fluorescence intensity of each image was analyzed by Image Pro Plus software. Their photostability was expressed by the ratio of the fluorescence intensity after excitation for a designated time interval to its initial value as a function of the exposure time.

Acknowledgements

The authors are grateful to Temasek Defence Systems Institute (ARF R-279-000-305-592/422/232), Singapore Ministry of Defense (R279-000-340-232), Singapore National Research Foundation (R279-000-390-281), and JCO-Astar (IMRE/12-8P1103) for financial support. Mr J. Geng thanks the National University of Singapore for a research scholarship.

Notes and references

1 T. G. Ksiazek, D. Erdman, C. S. Goldsmith, S. R. Zaki, T. Peret, S. Emery, S. X. Tong, C. Urbani, J. A. Comer, W. Lim, P. E. Rollin, S. F. Dowell, A. E. Ling, C. D. Humphrey, W. J. Shieh, J. Guarner, C. D. Paddock, P. Rota, B. Fields, J. DeRisi, J. Y. Yang, N. Cox, J. M. Hughes, J. W. LeDuc, W. J. Bellini, L. J. Anderson and S. W. Grp, *N. Engl. J. Med.*, 2003, **348**, 1953; I. L. Medintz, H. T. Uyeda, E. R. Goldman and H. Mattoussi, *Nat. Mater.*, 2005, **4**, 435.

2 M. Bai and D. J. Bornhop, *Curr. Med. Chem.*, 2012, **19**, 4742.

3 J. Lippincott-Schwartz, E. Snapp and A. Kenworthy, *Nat. Rev. Mol. Cell Biol.*, 2001, **2**, 444; X. H. Gao, Y. Y. Cui, R. M. Levenson, L. W. K. Chung and S. M. Nie, *Nat. Biotechnol.*, 2004, **22**, 969.

4 U. Resch-Genger, M. Grabolle, S. Cavaliere-Jaricot, R. Nitschke and T. Nann, *Nat. Methods*, 2008, **5**, 763; X. H. Gao, L. L. Yang, J. A. Petros, F. F. Marshal, J. W. Simons and S. M. Nie, *Curr. Opin. Biotechnol.*, 2005, **16**, 63.

5 A. M. Smith, H. W. Duan, A. M. Mohs and S. M. Nie, *Adv. Drug Delivery Rev.*, 2008, **60**, 1226; N. Lewinski, V. Colvin and R. Drezek, *Small*, 2008, **4**, 26; T. Jamieson, R. Bakhshi, D. Petrova, R. Pocock, M. Imani and A. M. Seifalian, *Biomaterials*, 2007, **28**, 4717.

6 K.-Y. Pu and B. Liu, *Adv. Funct. Mater.*, 2011, **21**, 3408.

7 C. L. Zhu, L. B. Liu, Q. Yang, F. T. Lv and S. Wang, *Chem. Rev.*, 2012, **112**, 4687.

8 X. L. Feng, L. B. Liu, S. Wang and D. B. Zhu, *Chem. Soc. Rev.*, 2010, **39**, 2411.

9 A. S. W. Thomas, G. D. Joly and T. M. Swager, *Chem. Rev.*, 2007, **107**, 1339; D. T. McQuade, A. E. Pullen and T. M. Swager, *Chem. Rev.*, 2000, **100**, 2537; B. Liu and G. C. Bazan, *Chem. Mater.*, 2004, **16**, 4467; G. X. Feng, D. Ding and B. Liu, *Nanoscale*, 2012, **4**, 6150; J. L. Geng, L. Zhou and B. Liu, *Chem. Commun.*, 2013, **49**, 4818–4820; A. Duarte, K. Y. Pu, B. Liu and G. C. Bazan, *Chem. Mater.*, 2011, **23**, 501; T. L. Kelly and M. O. Wolf, *Chem. Soc. Rev.*, 2010, **39**, 1526.

10 K. Li and B. Liu, *J. Mater. Chem.*, 2012, **22**, 1257.

11 J. Liu, D. Ding, J. L. Geng and B. Liu, *Polym. Chem.*, 2012, **3**, 1567.

12 V. Ibrahimova, S. Ekiz, O. Gezici and D. Tuncel, *Polym. Chem.*, 2011, **2**, 2818.

13 E.-J. Park, T. Erdem, V. Ibrahimova, S. Nizamoglu, H. V. Demir and D. Tuncel, *ACS Nano*, 2011, **5**, 2483; L. Zhou, J. L. Geng, G. Wang, J. Liu and B. Liu, *ACS Macro Lett.*, 2012, **1**, 927.
14 C. Wu, B. Bull, C. Szymanski, K. Christensen and J. McNeill, *ACS Nano*, 2008, **2**, 2415; Z. Hashim, P. Howes and M. Green, *J. Mater. Chem.*, 2011, **21**, 1797.
15 C. Wu, C. Szymanski, Z. Cain and J. McNeill, *J. Am. Chem. Soc.*, 2007, **129**, 12904.
16 J. L. Geng, K. Li, K. Y. Pu, D. Ding and B. Liu, *Small*, 2012, **8**, 2421; J. L. Geng, K. Li, W. Qin, L. Ma, G. G. Gurzadyan, B. Z. Tang and B. Liu, *Small*, 2013, **9**, 2012.
17 P. Howes, M. Green, A. Bowers, D. Parker, G. Varma, M. Kallumadil, M. Hughes, A. Warley, A. Brain and R. Botnar, *J. Am. Chem. Soc.*, 2010, **132**, 9833.
18 P. Howes, M. Green, J. Levitt, K. Suhling and M. Hughes, *J. Am. Chem. Soc.*, 2010, **132**, 3989.
19 K. Li, J. Pan, S.-S. Feng, A. W. Wu, K.-Y. Pu, Y. Liu and B. Liu, *Adv. Funct. Mater.*, 2009, **19**, 3535.
20 J. E. Lee, N. Lee, T. Kim, J. Kim and T. Hyeon, *Acc. Chem. Res.*, 2011, **44**, 893; L. Wang and W. H. Tan, *Nano Lett.*, 2006, **6**, 84; J. L. Geng, P. Liu, B. H. Liu, G. J. Guan, Z. P. Zhang and M. Y. Han, *Chem.–Eur. J.*, 2010, **16**, 3720; S. Bonacchi, D. Genovese, R. Juris, M. Montalti, L. Prodi, E. Rampazzo and N. Zaccheroni, *Angew. Chem., Int. Ed.*, 2011, **50**, 4056; F. Mahtab, J. W. Y. Lam, Y. Yu, J. Z. Liu, W. Z. Yuan, P. Lu and B. Z. Tang, *Small*, 2011, **7**, 1448.
21 S. Santra, P. Zhang, K. M. Wang, R. Tapec and W. H. Tan, *Anal. Chem.*, 2001, **73**, 4988.
22 A. Burns, P. Sengupta, T. Zedayko, B. Baird and U. Wiesner, *Small*, 2006, **2**, 723.
23 A. Burns, H. Ow and U. Wiesner, *Chem. Soc. Rev.*, 2006, **35**, 1028.
24 H. Tan, Y. Zhang, M. Wang, Z. X. Zhang, X. H. Zhang, A. M. Yong, S. Y. Wong, A. Y. C. Chang, Z. K. Chen, X. Li, M. Choolani and J. Wang, *Biomaterials*, 2012, **33**, 237.
25 R. Ravindranath, P. K. Ajikumar, N. B. Muhammad Hanafiah, W. Knoll and S. Valiyaveettil, *Chem. Mater.*, 2006, **18**, 1213; T. L. Kelly, Y. Yamada, C. Schneider, K. Yano and M. O. Wolf, *Adv. Funct. Mater.*, 2009, **19**, 3737; R. C. Evans, A. G. Macedo, S. Pradhan, U. Scherf, L. D. Carlos and H. D. Burrows, *Adv. Mater.*, 2010, **22**, 3032; F. Cucinotta, F. Carniato, G. Paul, S. Bracco, C. Bisio, S. Caldarelli and L. Marchese, *Chem. Mater.*, 2011, **23**, 2803.
26 B. Liu, B. S. Gaylord, S. Wang and G. C. Bazan, *J. Am. Chem. Soc.*, 2003, **125**, 6705; C. Wang, R. Y. Zhan, K. Y. Pu and B. Liu, *Adv. Funct. Mater.*, 2010, **20**, 2597; B. Liu and G. C. Bazan, *J. Am. Chem. Soc.*, 2004, **126**, 1942; J. Liu, J. Geng and B. Liu, *Chem. Commun.*, 2013, **49**, 1491.
27 B. Y. S. Kim, J. T. Rutka and W. C. W. Chan, *N. Engl. J. Med.*, 2010, **363**, 2434.
28 D. Peer, J. M. Karp, S. Hong, O. C. FaroKhzad, R. Margalit and R. Langer, *Nat. Nanotechnol.*, 2007, **2**, 751.
29 W. Schartl, *Nanoscale*, 2010, **2**, 829.
30 R. G. Chaudhuri and S. Paria, *Chem. Rev.*, 2012, **112**, 2373; S. H. Liu and M. Y. Han, *Adv. Funct. Mater.*, 2005, **15**, 961.
31 H. Nakajima, N. Mizuta, K. Sakaguchi, I. Fujiwara, A. Yoshimori, S. Takahashi, R. Takasawa and S. Tanuma, *Breast Cancer*, 2008, **15**, 65.
32 N. D. Hammer, S. Lee, B. J. Vesper, K. M. Elseth, B. M. Hoffman, A. G. M. Barrett and J. A. Radosevich, *J. Med. Chem.*, 2005, **48**, 8125; J. F. Jin, Y. J. Gu, C. W. Y. Man, J. P. Cheng, Z. H. Xu, Y. Zhang, H. S. Wang, V. H. Y. Lee, S. H. Cheng and W. T. Wong, *ACS Nano*, 2011, **5**, 7838; K. A. Mahmoud, J. A. Mena, K. B. Male, S. Hrapovic, A. Kamen and J. H. T. Luong, *ACS Appl. Mater. Interfaces*, 2010, **2**, 2924.
33 J. L. Geng, K. Li, D. Ding, X. H. Zhang, W. Qin, J. Z. Liu, B. Z. Tang and B. Liu, *Small*, 2012, **8**, 3655.
34 K. Aslan and C. D. Geddes, *Chem. Soc. Rev.*, 2009, **28**, 2556; J. L. Geng, J. Liang, Y. S. Wang, G. G. Gurzadyan and B. Liu, *J. Phy. Chem. B*, 2011, **115**, 3281; J. R. Lakowicz, K. Ray, M. Chowdhury, H. Szmacinski, Y. Fu, J. Zhang and K. Nowaczyk, *Analyst*, 2008, **133**, 1308.
35 J. Kim, H. S. Kim, N. Lee, T. Kim, H. Kim, T. Yu, I. C. Song, W. K. Moon and T. Hyeon, *Angew. Chem., Int. Ed.*, 2008, **47**, 8438.
36 M. Y. Hu, L. Li, H. Wu, Y. Su, P. Y. Yang, M. Uttamchandani, Q. H. Xu and S. Q. Yao, *J. Am. Chem. Soc.*, 2011, **133**, 12009.